Vol 18 No 11, November 2009
1674-1056/2009/18(11)/4944-05

Chinese Physics B

© 2009 Chin. Phys. Soc.
and IOP Publishing Ltd

Crystal structure and magnetic properties of $Nd(Mn_{1-x}Fe_x)_2Si_2$ compounds*

Chen Ye-Qing(陈业青)[a], Luo Jun(骆 军)[a]†, Liang Jing-Kui(梁敬魁)[a,b], Li Jing-Bo(李静波)[a], and Rao Guang-Hui(饶光辉)[a]

[a] *Beijing National Laboratory for Condensed Matter Physics, Institute of Physics, Chinese Academy of Sciences, Beijing* 100190, *China*

[b] *International Center for Materials Physics, Chinese Academy of Sciences, Shenyang* 110016, *China*

(Received 25 May 2009; revised manuscript received 22 June 2009)

X-ray powder diffraction, resistivity and magnetization studies have been performed on polycrystalline $Nd(Fe_xMn_{1-x})_2Si_2$ ($0 \leq x \leq 1$) compounds which crystallize in a $ThCr_2Si_2$-type structure with the space group $I4/mmm$. The field-cooled temperature dependence of the magnetization curves shows that, at low temperatures, $NdFe_2Si_2$ is antiferromagnetic, while the other compounds show ferromagnetic behaviour. The substitution of Fe for Mn leads to a decrease in lattice parameters a, c and unit-cell volume V. The Curie temperature of the compounds first increases, reaches a maximum around $x = 0.7$, then decreases with Fe content. However, the saturation magnetization decreases monotonically with increasing Fe content. This Fe concentration dependent magnetization of $Nd(Fe_xMn_{1-x})_2Si_2$ compounds can be well explained by taking into account the complex effect on magnetic properties due to the substitution of Mn by Fe. The temperature's square dependence on electrical resistivity indicates that the curve of $Nd(Fe_{0.6}Mn_{0.4})_2Si_2$ has a quasi-linear character above its Curie temperature, which is typical of simple metals.

Keywords: $Nd(Fe_xMn_{1-x})_2Si_2$, crystal structure, magnetic properties, resistivity

PACC: 6110M, 6155H, 7220N

1. Introduction

Much attention has been focused on ternary RT_2M_2 compounds (R = rare earth, T = 3d transition metal, M = Si or Ge) due to their unique physical properties, such as superconductivity and heavy fermion behaviour.[1] Most of these compounds crystallize in a body-centred tetragonal $ThCr_2Si_2$-type structure with the space group $I4/mmm$. In each unit cell, there are 10 atoms, i.e. $Z = 2$. The $ThCr_2Si_2$-type compound has a layered structure with $\ldots R-M-T_2-M-R-M-T_2-M-R\ldots$ planes (the so-called '$BaAl_4$' slab) stacked along the c-axis. Their atomic positions are as follows: R at 2a (0, 0, 0), T at 4d (0, 1/2, 1/4) and M at 4e (0, 0, z) with z always close to 0.37. Consequently, the distances between the atoms mainly depend on the a- and c-parameters,[2] which is favourable for analysis of the magnetic properties of these compounds based on the T–T distance.

According to the previous neutron diffraction investigation, the magnetic structure of $NdFe_2Si_2$ consists of ferromagnetic sheets perpendicular to c with the magnetic axis along c. These sheets are stacked according to the sequence $++--$, yielding doubling of the c axis. The Néel temperature, $T_N \sim 15.6$ K, was determined from the intensity–temperature curve of the strongest superlattice line.[3] Single crystal experiments performed by Sechovský *et al*[4] showed that the $NdFe_2Si_2$ were antiferromagnetic alloys ordered below the Néel temperature $T_N = 13.7$ K and had a uniaxial magnetocrystalline anisotropy with the easy magnetization direction along the c-axis. It is notable that the Fe atom is nonmagnetic in RFe_2X_2 compounds. Even doped into the magnetic compound RMn_2X_2, Fe still behaves as a nonmagnetic element.[5]

The RMn_2X_2 compounds form a distinct group, unlike other transition metals, since the magnetic coupling of the Mn sublattice is much more complicated.[1] The Mn–Mn exchange interaction is very sensitive to the intralayer Mn–Mn distance (d^a_{Mn-Mn}). It has been reported that if $d^a_{Mn-Mn} > 2.87$ Å ($a \sim 4.06$ Å), the Mn moments are canted. The intralayer (in-plane) Mn–Mn coupling is antiferromagnetic, while the interlayer (along the c axis) Mn–Mn coupling is ferromagnetic. When $2.84 < d^a_{Mn-Mn} < 2.87$ Å ($\sim 4.02 < a <\sim 4.06$ Å), the Mn moments are

*Project supported by the National Basic Research Program of China (Grant No 2006CB601101).

†Corresponding author. E-mail: jluo@aphy.iphy.ac.cn

also canted, but both the intralayer and interlayer couplings are antiferromagnetic. For $d^a_{Mn-Mn} < 2.84$ Å ($a < 4.02$ Å), the Mn sublattice is collinear ferromagnetic (light rare earth compound) or antiferromagnetic (heavy rare earth compound) along the c-axis.[6−15] As for the $NdMn_2Si_2$ compound, the Nd sublattice is ferromagnetic and the Mn sublattice is canted ferromagnetic along the c-axis at low temperature, and the $NdMn_2Si_2$ compound is also ferromagnetic below its Curie temperature $T_C = 34$ K due to the ferromagnetic coupling of the two sublattices. Above T_C, the Mn sublattice is collinear antiferromagnetic and the Nd sublattice becomes disordered, leading to the antiferromagnetic behaviour of the $NdMn_2Si_2$ compound. As the temperature increases, the $NdMn_2Si_2$ compound shows paramagnetic above its Neel temperature $T_N = 382$ K.[16,17] The $NdFe_2Si_2$ and $NdMn_2Si_2$ compounds show interesting magnetic properties and exotic magnetic phase transitions.[18,19] In this paper, we present the influence of substitution of Fe for Mn on the crystal structure and magnetic properties of $Nd(Fe_xMn_{1-x})_2Si_2$ ($0 \le x \le 1$) compounds.

2. Experimental

The $Nd(Fe_xMn_{1-x})_2Si_2$ samples with $0 \le x \le 1$ (interval 0.1) were prepared by arc melting on a water-cooled copper crucible with a non-consumable tungsten electrode under a high purity argon atmosphere. The purity of the elements was 99.98% for Mn and Fe, 99.9% for Nd, and 99.99% for Si. The mass loss of Mn during the melting was compensated by adding 10% excess Mn. The ingots were turned over and re-melted several times in order to achieve complete fusion and good homogeneity. Subsequently the sample was annealed in an evacuated quartz tube at 900°C for 2 weeks.

The x-ray powder diffraction (XRD) patterns of the compounds were collected at room temperature using a Rigaku D/Max 2500 diffractometer with CuKα radiation and graphite monochromator operated at 44 kV and 250 mA. The scan range was from 10° to 110° (2θ) with a step size of 0.02° and a sampling time of 1 s. XRD profile fitting was performed using the DBWS9807a[20] program. The temperature dependence of the magnetization (M) of the samples was measured on a superconducting quantum interference device (SQUID) magnetometer at a low field (500 Oe, 1 Oe = 79.5775 A/m) in the temperature range from 5 K to 300 K. The field-dependent magnetization and hysteresis loop were measured at 5 K in fields up to 50 kOe. The electrical resistivity was measured in the temperature range from 5 to 300 K by a standard four-probe method with a voltage resolution of 10^{-7} V and a current of 18 mA.

3. Results and discussion

The XRD patterns in Fig.1 show that single phase $Nd(Fe_xMn_{1-x})_2Si_2$ samples with a $ThCr_2Si_2$-type structure have been synthesized. With the increase of the Fe content, the Bragg reflection of the XRD pattern shifts towards higher angles. This indicates that the lattice constants decrease with Fe concentration since the atomic radius of Fe is smaller than that of Mn. All the XRD data have been analysed by the Rietveld refinement program DBWS9807a.[20] The observed, calculated and residuals of the XRD pattern of $Nd(Fe_xMn_{1-x})_2Si_2$ ($x = 0.5$) are shown in Fig.2 as an example.

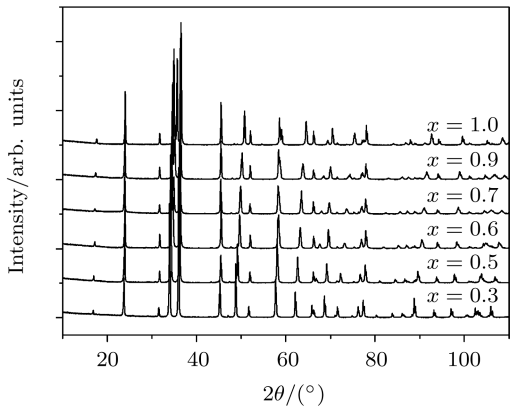


Fig.1. XRD patterns of $Nd(Fe_xMn_{1-x})_2Si_2$ samples.

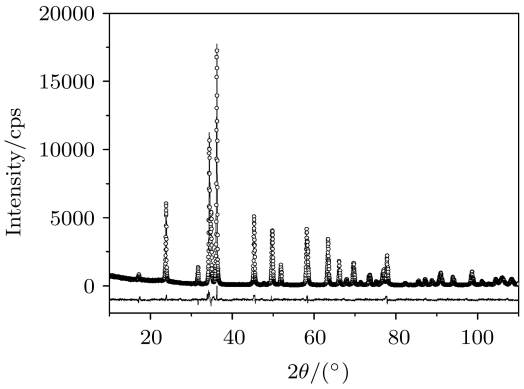


Fig.2. The observed, calculated and residuals of the XRD of $Nd(Fe_xMn_{1-x})_2Si_2$ ($x = 0.5$). The circles and continuous lines correspond to the experimental and calculated patterns respectively. The bottom curve depicts the difference between the experimental and calculated intensities.

As shown in Table 1 and Fig.3, both the lattice parameter and unit cell volume decrease almost linearly with increasing Fe concentration, but the atomic parameter $Z_{\rm Si}$ is almost constant (0.373 ± 0.003) for all compounds, which is very close to the ideal interlayer distance ($Z_{\rm Si} = 3/8$) for this type of structure. The calculated intralayer Mn–Mn distance $d_{\rm Mn-Mn}$ of $Nd(Fe_xMn_{1-x})_2Si_2$ decreases from 2.8361 for $x = 0$ to 2.8197 Å for $x = 0.9$ and the Fe–Fe distance is 2.8180 Å for $x = 1.0$.

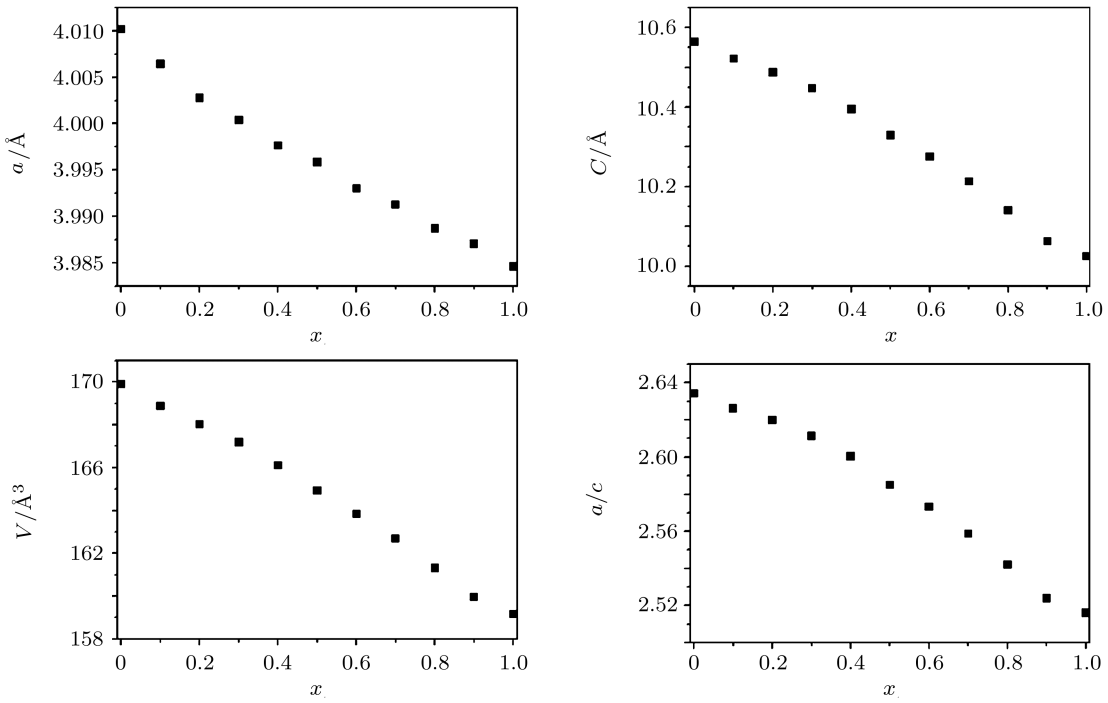


Fig.3. The lattice constants a and c, unit cell V, and the a/c ratio of $Nd(Fe_xMn_{1-x})_2Si_2$ as a function of Fe content x.

Table 1. The structural parameters derived from Rietveld refinements of the XRD patterns of $Nd(Fe_xMn_{1-x})_2Si_2$ compounds.

x	a/Å	c/Å	V/Å^3	c/a	$d_{\rm Mn-Mn}$/Å	$R_{\rm P}$%	R_{WP}/%	Z(Si site)
0	4.0102(0)	10.563(6)	169.88(0)	2.634	2.8361	11.43	15.05	0.373
0.1	4.0064(0)	10.521(2)	168.88(2)	2.626	2.8334	10.64	13.78	0.374
0.2	4.0027(1)	10.487(2)	168.02(1)	2.620	2.8308	12.86	16.31	0.376
0.3	4.0003(2)	10.446(4)	167.17(5)	2.611	2.8291	12.11	15.61	0.375
0.4	3.9976(2)	10.395(2)	166.12(0)	2.600	2.8272	11.82	15.23	0.374
0.5	3.9958(4)	10.328(4)	164.91(1)	2.585	2.8259	12.34	15.57	0.371
0.6	3.9930(3)	10.275(2)	163.82(4)	2.573	2.8239	12.28	15.51	0.372
0.7	3.9913(2)	10.212(4)	162.69(4)	2.559	2.8227	11.95	15.34	0.374
0.8	3.9887(1)	10.139(6)	161.32(0)	2.542	2.8209	10.78	13.83	0.373
0.9	3.9870(4)	10.063(2)	159.96(3)	2.524	2.8197	11.54	15.21	0.375
1.0	3.9846(2)	10.025(2)	159.17(2)	2.516	2.8180	12.01	15.27	0.373

The field-cooled (FC) $M(T)$ curves of the samples with $x = 1$, 0.9, 0.7, 0.6, 0.5 and 0.3, collected in a field of 500 Oe, are shown in Fig.4. At low temperatures, $NdFe_2Si_2$ is antiferromagnetic with $T_{\rm N} = 13.6$ K, agreeing well with the literature,[1] while the other compounds show ferromagnetic behaviour at low temperatures. The

Curie temperatures T_C of these compounds have been determined by plotting the M^2–T curves and extrapolating M^2 to zero, and are 19.3, 26.7, 41.8, 45.9, and 24.7 K for $x = 0.3$, 0.5, 0.6, 0.7, and 0.9, respectively. The dependence of T_C on the Fe content is illustrated in the inset of Fig.4. On the one hand, the substitution of Fe for Mn results in an enhancement of the Mn–Mn exchange interaction due to the decrease of the Mn–Mn distance. Therefore, the Curie temperature first increases with the Fe content. On the other hand, as mentioned above, Fe behaves as a nonmagnetic element in the RFe_2X_2 compounds.[5] With the further increase of the Fe content, the Curie temperature decreases due to the magnetic dilution effect of Fe. Therefore, the competition between the enhancement of the Mn–Mn exchange interaction and magnetic dilution effect causes the Curie temperature to increase initially, and reach a maximum at $x = 0.7$, then decrease with Fe content.

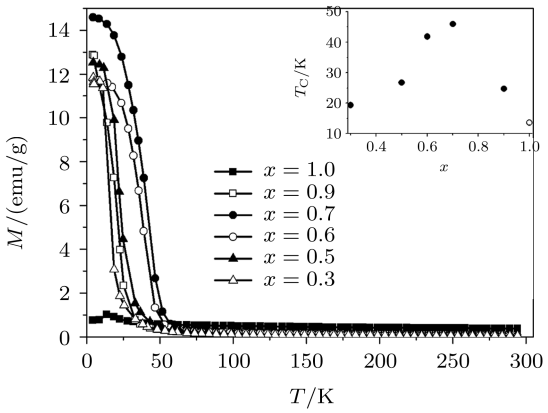


Fig.4. Temperature dependence of the magnetization of $Nd(Fe_xMn_{1-x})_2Si_2$ with $x = 1$, 0.9 0.7, 0.6, 0.5 and 0.3 in a field of 500 Oe. Inset shows the dependence of the Curie temperature on the Fe concentration (solid circles), and the open circle denotes the Neel temperature for $x = 1.0$.

Magnetization versus applied field (M–H) curves, recorded at 5 K in fields up to 5 T, are shown in Fig.5. The M–H curves show a curvature at low fields, which is characteristic of a ferromagnetic domain effect. The saturation magnetization M_S at 5 K is derived from the M versus $1/H$ plots by extrapolating $1/H$ to zero according to the law of approach to saturation. As shown in the inset of Fig.5, the saturation magnetization M_S decreases with increasing Fe content due to the magnetic dilution effect of the nonmagnetic Fe.

Figure 6 shows the hysteresis loop measured at 5 K for $Nd(Fe_{0.6}Mn_{0.4})_2Si_2$, which clearly indicates the ferromagnetic feature of the compound. The remanence ratio (M_r/M_s) at 5 K is found to be ∼66% and the intrinsic coercivity is as large as 15.1 kOe, which indicates the hard magnetic feature of $Nd(Fe_{0.6}Mn_{0.4})_2Si_2$ at 5 K.

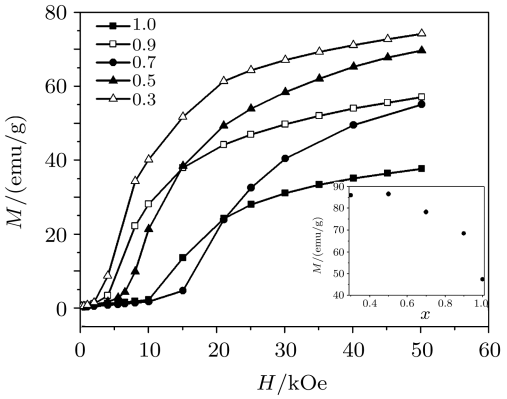


Fig.5. Magnetization curves of the $Nd(Fe_xMn_{1-x})_2Si_2$ with $x = 1$, 0.9 0.7, 0.5 and 0.3 at 5 K. Inset shows the dependence of the saturation magnetization on the Fe concentration.

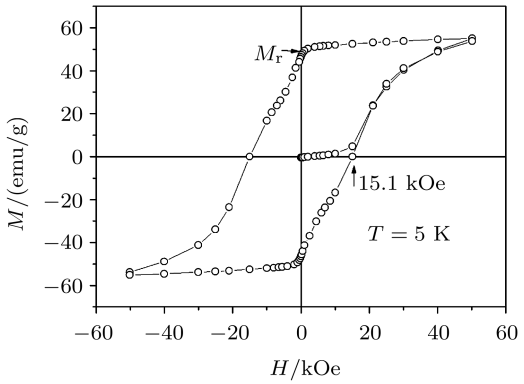


Fig.6. Hysteresis loop of $Nd(Fe_{0.6}Mn_{0.4})_2Si_2$ at 5 K.

The temperature's square (T^2) dependence on the electrical resistivity $\rho(T)$ of $Nd(Fe_{0.6}Mn_{0.4})_2Si_2$ in the 5–300 K temperature range is shown in Fig.7. The distinct kink at $T = 23.2$ K agrees well with the Curie

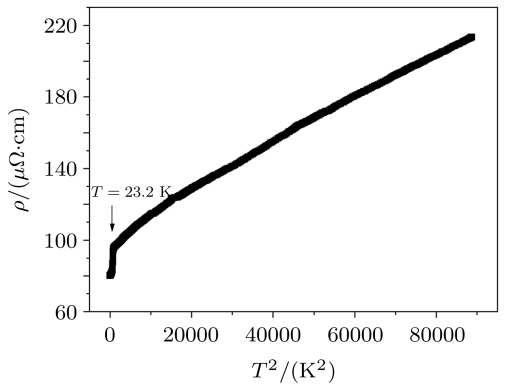


Fig.7. The temperature's square dependence on the electrical resistivity $\rho(T)$ of $Nd(Fe_{0.6}Mn_{0.4})_2Si_2$ in the temperature range of 5–300 K.

temperature of $Nd(Fe_{0.6}Mn_{0.4})_2Si_2$. The quasi-linear character of the $\rho(T)$ curve above the ordering temperature reflects the fact that the compound is typical of simple metals.

4. Conclusions

All $Nd(Fe_xMn_{1-x})_2Si_2$ compounds crystallize in a $ThCr_2Si_2$-type structure with the space group $I4/mmm$. The magnetic properties of polycrystalline samples have been studied by the field and temperature dependence of magnetization. The field-cooled (FC) $M(T)$ curves show that the studied compounds have ferromagnetic order. The Curie temperature increases with Fe content up to $x = 0.7$ then decreases, while the saturation magnetization decreases monotonically with increasing Fe content. The Fe concentration dependence on the magnetic properties of the $Nd(Fe_xMn_{1-x})_2Si_2$ compounds is explained based on the enhancement of the Mn–Mn exchange interaction due to the decrease of the Mn–Mn distance and the magnetic dilution effect of the nonmagnetic Fe. T^2 dependence on electrical resistivity indicates that the compound is typical of simple metals above its ordering temperature.

References

[1] Szytula A and Leciejewicz J In: Gschneidner Jr K A and Eyring L (eds.) 1989 *Handbook on the Physics and Chemistry of Rare Earths* **12** 133

[2] Ban Z and Sikirica M 1965 *Acta Crystallogr.* **18** 594

[3] Pinto H and Shaked H 1973 *Phys. Rev.* B **7** 3261

[4] Vejpravová J, Svoboda P and Sechovský V 2004 *J. Magn. Magn. Mater.* **272-276** 587

[5] Nowik I, Levi Y, Felner I and Bauminger E R 1995 *J. Magn. Magn. Mater.* **147** 373

[6] Kervan S, Elerman Y and Acet M 2002 *J. Alloy Comp.* **335** 70

[7] Kilic A, Kervan S, Özcan and Gencer A 2005 *J. Magn. Magn. Mater.* **288** 244

[8] Kervan S, Elerman Y and Acet M 2001 *J. Alloy Comp.* **321** 35

[9] Venturini G, Welter R, Ressouche E and Malaman B 1995 *J. Alloy Comp.* **224** 262

[10] Venturini G 1996 *J. Alloy Comp.* **232** 133

[11] Norlidah M N, Venturini G, Malaman B and Ressouche E 1996 *J. Alloy Comp.* **245** 80

[12] Norlidah M N, Venturini G, Malaman B and Ressouche E 1997 *J. Alloy Comp.* **248** 112

[13] Venturini G, Welter R, Ressouche E and Malaman B 1995 *J. Alloy Comp.* **223** 101

[14] Venturini G, Welter R, Ressouche E and Malaman B 1995 *J. Magn. Magn. Mater.* **150** 197

[15] Kumar P, Singh N K, Suresh K G, Nigam A K and Malik S K 2007 *J. Appl. Phys.* **101** 013908

[16] Welter R, Venturini G, Fruchart D and Malaman B 1993 *J. Alloy Comp.* **191** 263

[17] Szytula A and Szott I 1981 *Solid State Commun.* **40** 199

[18] Narasimhan K S V L, Rao V U S, Bergner R L and Wallace W E 1975 *J. Appl. Phys.* **46** 4957

[19] Kervan S, Elerman V and Acet M 2001 *Solid State Commun.* **119** 95

[20] Young R A, Larson A C and Paiva-Santos C O 1999 *User's Guide to Program DBWS-9807a for Rietveld Analysis of X-ray and Neutron Powder Diffraction Patterns with a PC and Various Other Computers,* School of Physics, Georgia Institute of Technology, Atlanta, Georgia,.